

# Enhanced Drug Delivery by Dissolution of Amorphous Drug Encapsulated in a Water Unstable Metal–Organic Framework (MOF)

Kuthuru Suresh and Adam J. Matzger\*

**Abstract:** Encapsulating a drug molecule into a water-reactive metal–organic framework (MOF) leads to amorphous drug confined within the nanoscale pores. Rapid release of drug occurs upon hydrolytic decomposition of MOF in dissolution media. Application to improve dissolution and solubility for the hydrophobic small drug molecules curcumin, sulindac, and triamterene is demonstrated. The drug@MOF composites exhibit significantly enhanced dissolution and achieves high supersaturation in simulated gastric and/or phosphate buffer saline media. This combination strategy where MOF inhibits crystallization of the amorphous phase and then releases drug upon MOF irreversible structural collapse represents a novel and generalizable approach for drug delivery of poorly soluble compounds while overcoming the traditional weakness of amorphous drug delivery: physical instability of the amorphous form.

Oral delivery is the preferred route for drug administration due to its convenience, high patient compliance, and cost-effectiveness. If drug dissolution is fast in the gastrointestinal tract, relatively rapid absorption and the accompanying onset of therapeutic activity is observed.<sup>[1]</sup> Achieving the desired concentration to facilitate drug absorption depends on solubility under physiological conditions, and poor aqueous solubility is a significant challenge in drug development and formulation. Drug candidates being generated in the R&D pipeline, and many currently marketed drugs, suffer from poor solubility.<sup>[2,3]</sup> A number of approaches for improving solubility have been pursued, such as amorphous solid dispersions using appropriate polymeric excipients,<sup>[4–6]</sup> cocrystallization,<sup>[7,8]</sup> and solubilization in co-solvents.<sup>[9]</sup> Although these approaches can improve performance relative to pure drugs, each has various drawbacks, mainly related to the chemical stability of the drug and physical stability against crystallization. Thus, there still is a need for methodologies to improve drug solubility with the ultimate goal being a general platform for amorphous drug stabilization during storage and administration. Here, a general approach to improve drug solubility is demonstrated by incorporating drugs into a metal–organic framework (MOF); the MOF acts as a drug carrier that inhibits crystallization of drug by confinement

within its nanoscale pores and yet undergoes rapid hydrolytic decomposition in simulated gastric (SG) and phosphate buffer saline (PBS) media leading to immediate release of an amorphous drug (Figure 1). This amorphous delivery system exhibits an increase in the free energy of drug relative to the crystalline form which is essential for generating high supersaturation. To our knowledge, this methodology for encapsulation and immediate release of pharmaceuticals has not been previously reported.

Current approaches employing MOFs in drug delivery center around controlled release.<sup>[10,11]</sup> For example, MOFs have been demonstrated to be excellent candidates for micro/nanomedicine-extended or controlled cargo delivery.<sup>[12–16]</sup> In these delivery models, MOFs with long-term chemical stability in media serve as drug release regulators upon activation by diverse stimuli such as media pH, temperature or pressure.<sup>[10]</sup> MOFs using a slow drug release model are beneficial for moderate to high solubility compounds and may improve chemical stability<sup>[12–15]</sup> of molecules by limiting total exposure of the compound in the digestive tract. This approach competes with polymers used as drug delivery vehicles for controlled release.<sup>[17–20]</sup> In contrast, here the immediate release of an amorphous drug in aqueous media from a drug@MOF composite via MOF hydrolytic degradation is leveraged for enhancing drug dissolution and solubility; this approach represents a general platform for delivering poorly soluble drugs.

When considering an appropriate MOF to serve as an amorphous drug stabilizer and fast release host the major considerations are 1) acceptable toxicity profile, 2) reactive decomposition in appropriate media, and 3) suitable pore size to host drug targets. Based on these criteria, MOF-5 was selected as the host as it is built from zinc clusters and terephthalic acid.<sup>[21]</sup> Zinc is used in many dietary vitamin and mineral supplements, in which zinc exists as zinc oxide, zinc acetate or zinc gluconate. The organic linker terephthalic acid exhibits low toxicity and a very high safe oral dose (lethal dose, LD<sub>50</sub> over 1 g kg<sup>-1</sup> in a mouse model).<sup>[22,23]</sup> Most importantly, MOF-5 is unstable to hydrolysis due to cleavage of coordination bonds in humid environments.<sup>[24]</sup> The structure of MOF-5 exhibits large pores ( $\approx 12.5$  Å diameter) suitable for hosting small molecule therapeutics.<sup>[22]</sup> Poorly water-soluble drug candidates curcumin (CUR), sulindac (SUL), and triamterene (TAT) were selected as the guest molecules. CUR is a hydrophobic polyphenol with dimensions  $\approx 17.3 \times 6.9$  Å. CUR displays potential therapeutic benefits such as antioxidant, anti-tumor, anti-inflammatory, anti-malarial, anti-bacterial, anti-viral, anti-hyperglycemic activities and acts against Alzheimer's disease.<sup>[25,26]</sup> CUR suffers from poor aqueous solubility, which impairs oral

[\*] Dr. K. Suresh, Prof. A. J. Matzger  
Department of Chemistry and the Macromolecular Science and Engineering Program, University of Michigan  
930 North University Avenue, Ann Arbor, MI 48109-1055 (USA)  
E-mail: matzger@umich.edu

Supporting information and the ORCID identification number(s) for the author(s) of this article can be found under <https://doi.org/10.1002/anie.201907652>.

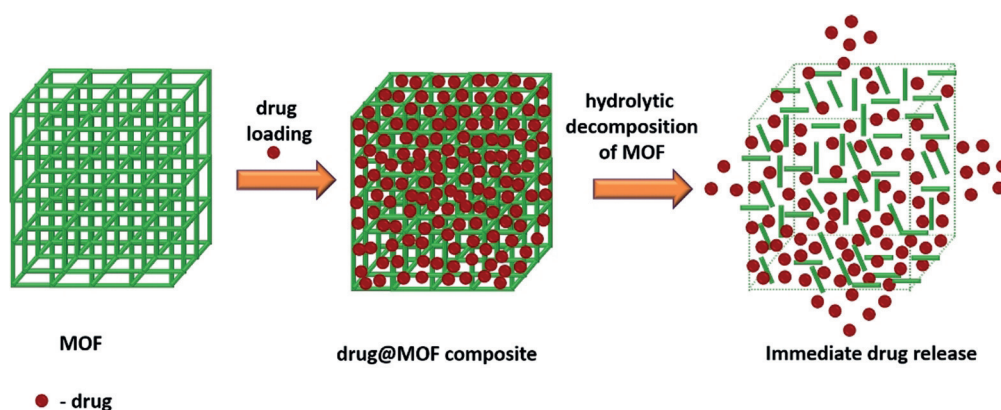


**Figure 1.** Schematic representation of a drug encapsulated into MOF followed by the immediate release of drug from drug@MOF composite via MOF hydrolytic decomposition.

bioavailability. SUL is a poorly soluble, non-steroidal anti-inflammatory drug with dimensions  $13.8 \times 7.6 \text{ \AA}$ .<sup>[27]</sup> TAT is a potassium-sparing diuretic drug with dimensions  $11.8 \times 7.6 \text{ \AA}$  that exhibits poor solubility.<sup>[28]</sup>

Drug molecules were encapsulated via post-synthetic incorporation by soaking activated MOF-5 crystals in excess of a drug in methylene chloride (for CUR) or acetonitrile (for SUL and TAT) (see Experimental section in the Supporting Information). The drug@MOF-5 composite crystals were removed by filtration and washed twice with the same solvent used for the incorporation to eliminate residual drug on the outside surface of MOF-5. The crystals were activated under vacuum. Optical microscopy (Figure 2a) shows the dramatic color change upon encapsulation of drug; CUR@MOF-5 is brick red and the SUL@MOF-5 and TAT@MOF-5 composites are yellow. Powder X-ray diffraction (PXRD) patterns of the composites demonstrate MOF-5 phase stability as crystallinity is retained after encapsulation of drug (Figure 2b and c). No diffraction peaks associated with drug molecules are observed, consistent with the pores being too small to support aggregation into a crystalline form. Proton NMR spectra of drug@MOF-5 composites, after digestion in acidic

[D<sub>6</sub>]DMSO, (see Figure S1, Supporting Information) reveal that the drugs do not degrade upon loading.

Host-guest interactions of drug@MOF-5 composites were analyzed using vibrational spectroscopy. Infrared (IR) and Raman spectra of drug@MOF-5 composites show strong similarities when compared to the crystalline starting components although peak shifts are evident in both host and guest (see Figures S2 and S3 and characteristic peaks listed in Table S1 in the Supporting Information). The IR spectrum of pure CUR exhibits a hydroxyl stretch at  $3510 \text{ cm}^{-1}$  which is shifted to lower frequency in CUR@MOF-5 ( $3509 \text{ cm}^{-1}$ ). The Raman spectrum of pure CUR contains a carbonyl stretch at  $1627 \text{ cm}^{-1}$  which is red shifted in CUR@MOF-5 to  $1626 \text{ cm}^{-1}$ . This contrasts with the blue shifting in pure amorphous CUR and is consistent with significant attractive drug-MOF interactions in the composite.<sup>[29]</sup> Shifting also occurs in the IR and Raman spectra of SUL when the molecule is incorporated into MOF-5. Red shifting of the carboxylic acid stretch at  $1697 \text{ cm}^{-1}$  to  $1677 \text{ cm}^{-1}$  in the IR spectrum and red shifting of peaks at  $1209$  and  $1118 \text{ cm}^{-1}$  (to  $1208$  and  $1115 \text{ cm}^{-1}$  respectively) in the Raman spectrum is observed and these results are mirrored in TAT@MOF-5. These data

are consistent with substantial attractive drug-MOF interactions in the composite which should contribute to long-term stability of amorphous phase against crystallization.

Weight percentage (wt%) of the incorporated drug in drug@MOF-5 composite was determined using UV-vis spectroscopy on digested samples (see Supporting Information). Drug encapsulation in MOF-5 was found to be 7.7 wt% for CUR, 22.4 wt% for SUL, and 34.0 wt% for TAT. This demonstrates 0.18 CUR, 0.61 SUL, and 1.61 TAT molecules per cage in MOF-5 were encapsulated, respectively (TAT encapsulated,

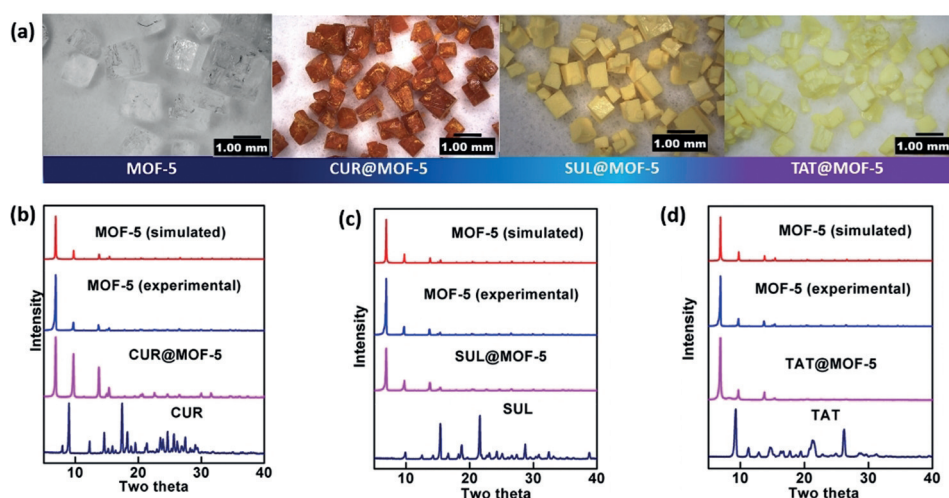


**Figure 2.** a) Optical images of MOF-5 and drug@MOF-5 composite crystals. b,c,d) PXRD patterns of drug@MOF-5 composites compared with their starting materials (MOF-5 and respective drug).

sulation in MOF-5 shown as an example in Figure 3). The achieved drug loading (wt%) for drug@MOF-5 composites are promising and comparable with drug-polymer solid dispersions, drug-polymer micelles, and nanomedicine-poly-

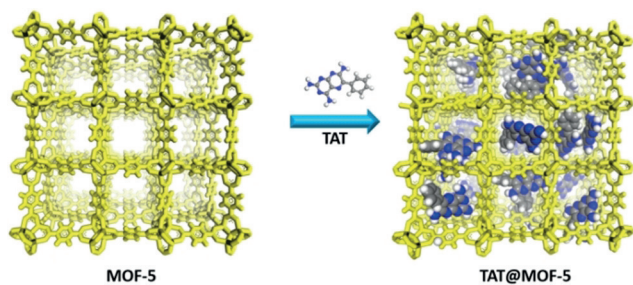


**Figure 3.** Illustration of the encapsulation of TAT drug into a MOF-5 (approx. two TAT molecules per cage were encapsulated in MOF-5).

mer composites where the drug loading is in range of  $\approx 5$  to 50% with respect to the carrier.<sup>[30–32]</sup> Furthermore, gas sorption analysis reveals that the BET surface area decreases in all the composites (CUR@MOF-5 ( $2777 \text{ m}^2 \text{ g}^{-1}$ ), SUL@MOF-5 ( $1969 \text{ m}^2 \text{ g}^{-1}$ ) and TAT@MOF-5 ( $550 \text{ m}^2 \text{ g}^{-1}$ )) relative to pure MOF-5 ( $3425 \text{ m}^2 \text{ g}^{-1}$ ) which shows that the pores of MOF-5 are occupied by drug molecules (see Figure S3, Supporting Information). This residual porosity follows the same trend as the wt% drug loading consistent with partial pore blockage; similar results were observed for polymer-MOF composites.<sup>[33]</sup> Residual porosity is important for allowing fast entry of water into the MOF to promote rapid framework degradation, although the tradeoff between porosity and drug loading must be optimized for each drug ultimately consistent with desired dosage and dissolution behavior.

To investigate host decomposition behavior, MOF-5 crystals were soaked in SG and PBS media at  $37^\circ\text{C}$ . The undissolved material from these media was determined by PXRD to be terephthalic acid in SG media, whereas a PBS media resulted in a Zn-terephthalate-dihydrate salt precipitate among other decomposition products<sup>[34]</sup> (see Figure S4, Supporting Information). The drug@MOF-5 composites exhibit decomposition behavior akin to pure MOF-5 (see Figure S5–S7, Supporting Information). Notably, SUL@MOF-5 decomposition in SG media resulted in SUL crystallized as form I (monoclinic) polymorph rather than as the more stable form II (orthorhombic); this finding is in accord with the Ostwald step rule.<sup>[35,36]</sup>

To determine drug dissolution rates and supersaturation generation from drug@MOF-5 composites, and from physical mixtures (PM), UV-vis spectroscopy was used to monitor the dissolution process at  $37^\circ\text{C}$  (Figures 4a–d and Table 1). Methyl cellulose was included in both dissolution media to inhibit precipitation of drug molecules at high supersaturation and to serve as a proxy for what would be an extensive formulation process of this supersaturating drug delivery system. The shape of the drug concentration vs. time curves for CUR@MOF-5 in both media indicates that CUR undergoes rapid dissolution and maintains high supersaturation.

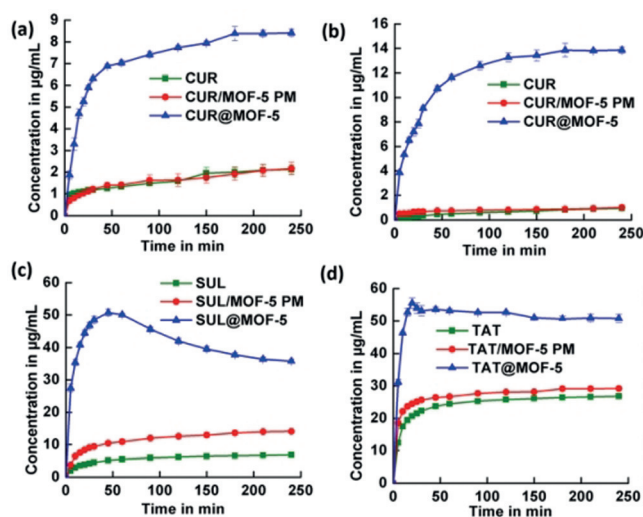


**Figure 4.** Representative CUR, CUR@MOF-5 and physical mixture (PM) dissolution profiles in (a) SG and (b) PBS media. c) Representative SUL, SUL@MOF-5, and SUL/MOF-5 PM dissolution profiles in SG media. d) Representative TAT, TAT@MOF-5 and TAT/MOF-5 PM dissolution profiles in PBS media.

**Table 1:** Representative drugs, drug@MOF-5 composites and their PM  $C_{\text{max}}$  and  $\text{AUC}_{0-4}$  values (average (standard error of the mean)) in SG and/or PBS media.

Compound	$C_{\text{max}}$ [ $\mu\text{g mL}^{-1}$ ]		$\text{AUC}_{0-4}$ [ $\text{mg h mL}^{-1}$ ]	
	SG media	PBS media	SG media	PBS media
CUR	2.12(21)	0.95(4)	0.39(6)	0.15(2)
CUR/MOF-5PM	2.16(3)	1.03(1)	0.39(6)	0.19(3)
CUR@MOF-5	8.45(19)	13.87 (27)	1.75(2)	2.88(4)
	SG media		SG media	
SUL	6.84(7)		1.38(2)	
SUL/MOF-5 PM	14.06(6)		2.83(5)	
SUL@MOF-5	50.73(41)		9.92(13)	
	PBS media		PBS media	
TAT	26.89(8)		5.89(9)	
TAT/MOF-5 PM	29.67(6)		8.74(9)	
TAT@MOF-5	55.50(2)		15.25(17)	

Immediate release of CUR molecules from CUR@MOF-5 via MOF hydrolytic decomposition leads to rapid dissolution which generates high supersaturation in the first 60 min. A maximum concentration ( $C_{\text{max}}$ ) of  $8.5 \mu\text{g mL}^{-1}$  in SG media and  $13.9 \mu\text{g mL}^{-1}$  in PBS media are observed and demonstrating that CUR@MOF-5 achieves a much higher CUR concentration upon dissolution than pure CUR. This immediate drug release from drug@MOF-5 composite is in contrast with controlled drug release from an amorphous drug@MOF composite with a water stable framework.<sup>[37]</sup> A CUR/MOF-5 PM displays a dissolution profile similar to pure CUR in both media, indicating that encapsulation is critical for performance. Moreover, CUR@MOF-5 achieves supersaturation significantly greater than that generated during the dissolution of CUR polymeric amorphous solid dispersions.<sup>[38]</sup>

Sulindac is a poorly water-soluble weak acid with pH-dependent solubility which exhibits a very low solubility in

SG media.<sup>[35]</sup> It is important to note that during dissolution of SUL@MOF-5 and SUL/MOF-5 PM in SG media, the pH slightly increases due to MOF-5 decomposition products. This change in the pH leads to substantial changes in SUL solubility. Immediate release of SUL from SUL@MOF-5 generates high supersaturation in the first 60 min of dissolution with a maximum concentration of  $50.7 \mu\text{g mL}^{-1}$ . As dissolution continues, the concentration of SUL declines slowly due to SUL precipitation from media. Nonetheless,  $C_{\text{max}}$  and AUC values of SUL@MOF-5 are much greater than pure SUL. Furthermore, SUL@MOF-5 achieves superior supersaturation as compared to SUL polymeric amorphous solid dispersions, which exhibit a  $C_{\text{max}}$  of  $<33 \mu\text{g mL}^{-1}$  in SG.<sup>[39]</sup>

Triamterene is a weakly basic drug that exhibits low solubility in neutral solutions and intestinal pH. Immediate release of TAT from TAT@MOF-5 generates high supersaturation in the first 20 min of dissolution with a maximum concentration of up to  $55.5 \mu\text{g mL}^{-1}$  which demonstrates that TAT@MOF-5 achieves enhanced concentration upon dissolution than pure TAT. A TAT/MOF-5 PM displays a dissolution profile similar to pure TAT.

Amorphous form stability is a critical problem in drug delivery, and we hypothesized that confinement in pores would block pharmaceutical crystallization indefinitely. Indeed, all the composites have good physical stability of more than 4 months in dry conditions at room temperature (see Figure S9, Supporting Information).

In conclusion, a new approach is demonstrated for enhancing the solubility of poorly soluble drugs using a water reactive MOF as a drug carrier. Encapsulating drug in MOF-5 to form a drug@MOF composite inhibits crystallization of amorphous phase drug (stable > 4 months) and facilitates immediate drug release in dissolution media upon hydrolytic MOF decomposition. The studied composites show fast drug release to generate high supersaturation, which offers the potential for enhanced drug absorption and rapid onset of therapeutic activity. The present supersaturating drug delivery system for immediate drug release formulations can be broadly applied to pharmaceutically acceptable water reactive MOFs and a large number of poorly soluble drug molecules as host-guest systems for enhancing drug solubility in a general fashion.

## Acknowledgements

This work was supported by the United States Department of Energy (DE-SC0004888).

## Conflict of interest

The authors declare no conflict of interest.

**Keywords:** amorphous drug · drug delivery · immediate drug release · metal-organic framework · stability

**How to cite:** *Angew. Chem. Int. Ed.* **2019**, *58*, 16790–16794  
*Angew. Chem.* **2019**, *131*, 16946–16950

- [1] D. D. Sun, P. I. Lee, *Mol. Pharm.* **2013**, *10*, 4330.
- [2] A. Fahr, X. Liu, *Expert Opin. Drug Delivery* **2007**, *4*, 403.
- [3] S. M. Paul, D. S. Mytelka, C. T. Dunwiddie, C. C. Persinger, B. H. Munos, S. R. Lindborg, A. L. Schacht, *Nat. Rev. Drug Discovery* **2010**, *9*, 203.
- [4] T. Vasconcelos, B. Sarmento, P. Costa, *Drug Discovery Today* **2007**, *12*, 1068.
- [5] K. Lehmkemper, S. O. Kyeremateng, O. Heinzerling, M. Degenhardt, G. Sadowski, *Mol. Pharm.* **2017**, *14*, 4374.
- [6] S. Baghel, H. Cathcart, N. J. O'Reilly, *J. Pharm. Sci.* **2016**, *105*, 2527.
- [7] C. B. Aakeröy, S. Forbes, J. Desper, *J. Am. Chem. Soc.* **2009**, *131*, 17048.
- [8] N. K. Duggirala, M. L. Perry, Ö. Almarsson, M. J. Zaworotko, *Chem. Commun.* **2016**, *52*, 640.
- [9] N. Seedher, M. Kanojia, *Pharm. Dev. Technol.* **2009**, *14*, 185.
- [10] M.-X. Wu, Y.-W. Yang, *Adv. Mater.* **2017**, *29*, 1606134.
- [11] P. Horcajada, T. Chalati, C. Serre, B. Gillet, C. Sebrie, T. Baati, J. F. Eubank, D. Heurtaux, P. Clayette, C. Kreuz, J.-S. Chang, Y. K. Hwang, V. Marsaud, P.-N. Bories, L. Cynober, S. Gil, G. Férey, P. Couvreur, R. Gref, *Nat. Mater.* **2009**, *9*, 172.
- [12] Z. Dong, Y. Sun, J. Chu, X. Zhang, H. Deng, *J. Am. Chem. Soc.* **2017**, *139*, 14209.
- [13] H. Zheng, Y. Zhang, L. Liu, W. Wan, P. Guo, A. M. Nyström, X. Zou, *J. Am. Chem. Soc.* **2016**, *138*, 962.
- [14] M. H. Teplensky, M. Fantham, P. Li, T. C. Wang, J. P. Mehta, L. J. Young, P. Z. Moghadam, J. T. Hupp, O. K. Farha, C. F. Kaminski, D. Fairen-Jimenez, *J. Am. Chem. Soc.* **2017**, *139*, 7522.
- [15] Y. Chen, P. Li, J. A. Modica, R. J. Drout, O. K. Farha, *J. Am. Chem. Soc.* **2018**, *140*, 5678.
- [16] W. J. Rieter, K. M. Taylor, W. Lin, *J. Am. Chem. Soc.* **2007**, *129*, 9852.
- [17] M. W. Tibbitt, J. E. Dahlman, R. Langer, *J. Am. Chem. Soc.* **2016**, *138*, 704.
- [18] K. E. Uhrich, S. M. Cannizzaro, R. S. Langer, K. M. Shakesheff, *Chem. Rev.* **1999**, *99*, 3181.
- [19] W. B. Liechty, D. R. Krysciold, B. V. Slaughter, N. A. Peppas, *Annu. Rev. Chem. Biomol. Eng.* **2010**, *1*, 149.
- [20] R. S. Langer, N. A. Peppas, *Biomaterials* **1981**, *2*, 201.
- [21] H. Li, M. Eddaoudi, M. O'Keeffe, O. M. Yaghi, *Nature* **1999**, *402*, 276.
- [22] R. J. Sheehan, *Ullmann's Encyclopedia of Industrial Chemistry*, Vol. 35, Wiley-VCH, Weinheim, **2005**, p. 639.
- [23] H. D. Heck, R. W. Tyl, *Regul. Toxicol. Pharmacol.* **1985**, *5*, 294.
- [24] P. Guo, D. Dutta, A. G. Wong-Foy, D. W. Gidley, A. J. Matzger, *J. Am. Chem. Soc.* **2015**, *137*, 2651.
- [25] K. Suresh, A. Nangia, *CrystEngComm* **2018**, *20*, 3277.
- [26] T. Esatbeyoglu, P. Huebbe, I. M. A. Ernst, D. Chin, A. E. Wagner, G. Rimbach, *Angew. Chem. Int. Ed.* **2012**, *51*, 5308; *Angew. Chem.* **2012**, *124*, 5402.
- [27] G. A. Shazly, *Biomed. Res. Int.* **2016**, *1*, 3182358.
- [28] W. J. Ma, J. M. Chen, L. Jiang, J. Yao, T. B. Lu, *Mol. Pharm.* **2013**, *10*, 4698.
- [29] P. Sanphui, N. R. Goud, U. B. R. Khandavilli, S. Bhanoth, A. Nangia, *Chem. Commun.* **2011**, *47*, 5013.
- [30] K. Kothari, V. Ragoonanan, R. Suryanarayanan, *Mol. Pharm.* **2015**, *12*, 1477.
- [31] S. Lv, Y. Wu, K. Cai, H. He, Y. Li, M. Lan, X. Chen, J. Cheng, L. Yin, *J. Am. Chem. Soc.* **2018**, *140*, 1235.
- [32] S. Çalıř, K. Öztürk, A. F. B. Arslan, H. Erođlu, Y. Çapan, *Nanocarriers for Drug Delivery*, Elsevier, Amsterdam, **2019**, chap. 4, p. 133.
- [33] N.-D. H. Gamage, K. A. McDonald, A. J. Matzger, *Angew. Chem. Int. Ed.* **2016**, *55*, 12099; *Angew. Chem.* **2016**, *128*, 12278.

- [34] K. A. Cychoz, A. J. Matzger, *Langmuir* **2010**, *26*, 17198.
- [35] A. L. Grzesiak, A. J. Matzger, *J. Pharm. Sci.* **2007**, *96*, 2978.
- [36] W. Ostwald, *Z. Phys. Chem.* **1897**, *22*, 289.
- [37] C. Orellana-Tavra, E. F. Baxter, T. Tian, T. D. Bennett, N. K. Slater, A. K. Cheetham, D. Fairen-Jimenez, *Chem. Commun.* **2015**, *51*, 13878.
- [38] S. Onoue, H. Takahashi, Y. Kawabata, Y. Seto, J. Hatanaka, B. Timmermann, S. Yamada, *J. Pharm. Sci.* **2010**, *99*, 1871.
- [39] J. Maclean, C. Medina, D. Daurio, F. Alvarez-Nunez, J. Jona, E. Munson, K. Nagapudi, *J. Pharm. Sci.* **2011**, *100*, 3332.

Manuscript received: June 19, 2019  
Version of record online: October 11, 2019

---